HIGH INITIAL BRAIN UPTAKE OF O-(2-([18]F)FLUOROETHYL)-D-TYROSINE (D-FET) IN PIGLETS

P. BRUST [1], S. FISCHER [1], V. MAKRIDES [2], R. BAUER [3], R. HINZ [4], K. HUGGEL [2], V. GANAPATHY [5], F. VERREY [2] and J. STEINBACH [1]

[1]Institute of Interdisciplinary Isotope Research, Leipzig, Germany; [2]Institute of Physiology, Zurich, Switzerland; [3]Institute of Molecular Cell Biology, Jena, Germany; [4]Wolfson Molecular Imaging Center, Manchester, United Kingdom; [5]Medical College of Georgia, Augusta, USA

Introduction: Although [^{18}F]FDG has been proven as the radioligand of choice for many extracranial tumors, radiolabeled amino acids are preferred for the study of intracerebral tumors with PET because transport mechanisms of large neutral amino acid (LNAA) are upregulated in those tumors. To overcome restrictions known for use of ^{11}C ^{18}F-labeled LNAA (e.g. L-FET) have been developed and used for this purpose. Recently experimental evidence has been obtained that D-enantiomers of some LNAA are superior to L-enantiomers with regard to the imaging of certain peripheral tumors. In this study, the transport of D-FET across the blood-brain barrier was studied with PET in piglets and compared with L-FET.

Experimental: Ten anesthetized piglets were intravenously infused with L-FET (98 ± 11 MBq, n=4) or D-FET (128 ± 34 MBq, n=6) in 10 ml saline. Compartmental modeling of PET data was used to estimate the rate constants for the blood-brain (K_1) and the brain-blood (k_2) transfer of both radiotracers. Additionally, two different approaches were used to assess the interaction of L-FET and D-FET with transporters known to have affinity for LNAA. First, we studied the hLAT1 transporter in HRPE cells (human retinal pigment epithelial cells). Second, hLAT1, LAT2, XPCT and PAT1 were studied in *Xenopus laevis* oocytes.

Results and Discussion: Our results reveal that the BBB transport of D-FET is significantly faster than that of L-FET. This finding is based on the following observations: (1) The normalized brain uptake in piglets of D-FET 5 min after injection is about 140% higher than that of L-FET. (2) The rate constants for the blood-brain and brain-blood transfer of D-FET in piglets are significantly higher (by factor 3-4) than those for L-FET. This stands in contrast with previous studies showing high and stereoselective uptake of L-FET in mouse brain. Thus, the transport kinetics for D-amino acids differs among species. The observed differences between L-FET and D-FET can only be explained by differences in their affinity to specific transport systems. L-FET showed at least 20-fold higher in vitro affinity than D-FET towards LAT1 and LAT2 whereas both enantiomers have similar affinities to XPCT and PAT1 transporters.

Conclusion: We have demonstrated specific transport of L-FET and D-FET across the BBB which cannot be fully explained by known transport systems. The study provides further evidence for the presence of an unknown, D-amino acid preferring transporter/transport system at the blood-brain barrier.

Keywords: Amino Acid Transport, Blood-Brain Barrier, Stereoselectivity, Tumor Imaging

NOVEL NANOCARRIERS FOR IMAGING AND DRUG DELIVERY: IN VIVO EVALUATION OF ^{64}Cu-LABELED PEG GRAFT COPOLYMERS

A. HAGOOLY [1], E.D. PRESSLY [2], R. ROSSIN [1], K. FUKUKAWA [2], B.A. MESSEMORE [2], C.J. HAWKER [2] and M.J. WELCH [1]

[1]Radiological Sciences, Washington University School of Medicine, St. Louis, MO, USA; [2]Materials Research Laboratory, University of California Santa Barbara, Santa Barbara, CA, USA

Introduction: There is a continuous effort to design nanocarriers for drug delivery as the ability of targeted nanoparticles (NPs) to deliver a payload in diseased tissues will improve the efficiency of treatment. To this aim, however, the NPs must avoid the RES and remain in the blood long enough. Herein, a series of novel graft copolymers (combs) containing different length PEG chains were investigated for this purpose. ^{64}Cu-labeling, biodistribution studies and microPET imaging were used to evaluate the pharmacokineticks of these agents in vivo.

Experimental: 1K (**1**), 2K (**2**) and 5K PEG (**3**) comb polymers were synthesized by RAFT polymerization [1], conjugated to DOTA and then collapsed in water to form NPs. After reaction with ^{64}Cu, the labeled NPs were purified by size exclusion chromatography (RCP > 95%, 10-20 mCi/mg) and administered in vivo. Biodistribution studies and small animal PET imaging were carried out in Sprague-Dawley rats (n = 4) and Balb/C mice (n = 1-3), respectively.

Results and Discussion: Fast and high uptake in the liver is a major obstacle for NPs in medical applications. To avoid this, surface PEG grafting is the most used approach [2]. Our data showed high blood uptake at 10 min p.i. (70-90%ID) for **1-3** and a strong correlation between the PEG length and the blood circulation time. In fact, **1** exhibited a fast clearance from the blood while **2** and **3** showed high blood retention up to 4 h p.i. (ca. 4.5%ID/g). At later time points, **2** cleared from the blood faster than **3** (0.7±0.1 and 2.2±0.2%ID/g at 48 h p.i. respectively). Noticeably, the liver showed an opposite trend compared to that of the blood confirming the key role of this organ in NP disposal. MicroPET imaging confirmed the biodistribution data. In fact, the heart of a mouse administered with **3** was clearly visible up to 24 h p.i. while the liver was the only lit up organ in mice administered with **1**. **2** exhibited an intermediate behavior.

Conclusion: Here we confirmed that ^{64}Cu and PET are excellent tools to evaluate NPs in vivo. Furthermore, we showed how the stealthiness of NPs can be influenced and the blood circulation can be modified by choosing the appropriate PEG graft on the NP. These experiments continue our efforts to develop NPs with optimal characteristics for nanomedicine applications.

Acknowledgement: This material is based upon work supported by the NIH as a Program of Excellence in Nanotechnology (HL080729). The production of ^{64}Cu is supported by a grant from the NCR (CA86307).

References: [1] S. Perrier *et al.*, *J. Polym. Sci. Part A: Polym, Chem.*, **43**, 5347-5393 (2005). [2] D.E. Owens III *et al.*, *Int. J. Pharm.*, **307**, 93-102 (2006).

Keywords: Biodistribution, MicroPET, 64-Cu, PEG, Nanoparticles

SCHIFF BASE DERIVATIVE FOR POSITRON EMISSION TOMOGRAPHY (PET) IMAGING OF AMYLOID IN BRAIN

J.M. ZHANG[1], Z. GUO[1], J.H. TIAN[1] and B.L. LIU[2]

[1]PET Center, The PLA General Hospital, Beijing, China; [2]Dept of Chemistry, Beijing Normal University, Beijing, China

Introduction: A variety of radiolabeled Congo red, Chrysamine-G, and stilbenes have been synthesized and evaluated as potential in vivo PET and SPECT imaging probes in AD brain. While many of these radiotracers had high affinity for A-beta, good brain uptake, fast washout. We reported the synthesis and initial characterization of Schiff base as amyloid imaging agent.

Experimental: Nine schiff base ligands(4-N,N-dimethylamino-4'-Schiff-X, X were –I,-F,NO_2,-OCH_3, -m-CH_3,-COOH,-$COOC_2H_5$ respectively) were synthesized by 4-X-aniline reaction with 4-(dimethylamino) benzaldehyde as candidates for amyloid imaging agent. The characters were confirmed by NMR.The schiff base derivative's binding affinity were measured with A-beta 40 aggregates in vitro binding assays. A novel probe,4'-Schiff-O[^{11}C]CH_3,was successfully prepared with [^{11}C]CH_3I (Fig. 1). Partition coefficient were measured.

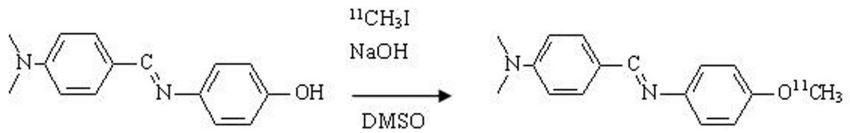

Fig. 1

Results and Discussion: The 4'-Schiff-OCH_3 showed high binding affinity to Ab40 aggregates (Ki=7.5nM). The 4'-Schiff-O[^{11}C]CH_3 was synthesis with yield of 75%. The compound was stable in base condition. The lipophilic of 4'-Schiff-O[^{11}C]CH_3 was expected to cross the intact BBB(Log PC=2.22), which a whole brain uptake of 6.45%ID/g at 2min post i.v. injection in normal mice and fast washout at 30min (1.70%ID/g). PET imaging studies in monkey was performed with 4'-Schiff-O[^{11}C]CH_3 (Fig. 2). At early time points, radioactivity appeared to accumulated at parietal lobe and occipital lobe, low uptake at white matter. At later times, the fast wash-out were seen in parietal and occipital, but white matter remained higher levels at 20min.

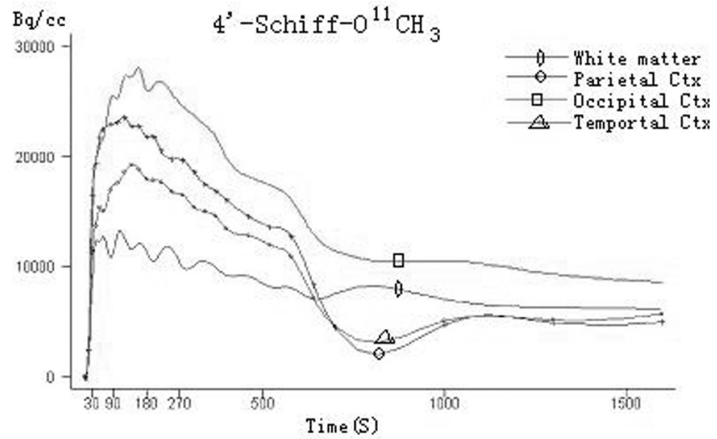

Fig. 2

Conclusion: It was sugguest that 4'-Schiff-O[^{11}C]CH_3 was a good candidate for imaging A -beta-amyloid depssits in vivo.

Keywords: Alzheimer's Diseases, Beta-Amyloid, Schiff Base, Carbon-11

PERIPHERAL METABOLISM OF *R*-([11]C)VERAPAMIL IN EPILEPSY PATIENTS

A. ABRAHIM[1], M. BAUER[1], G. LUURTSEMA[2], K. KLETTER[3], C. JOUKHADAR[1], C. BAUMGARTNER[4], M. MUELLER[1] and O. LANGER[1,5]

[1]Dept. of Clinical Pharmacology, Medical University of Vienna, Austria; [2]Nuclear Medicine & PET Research, VU University Medical Center, Amsterdam, Netherlands; [3]Dept. of Nuclear Medicine, Medical University of Vienna, Austria; [4]Dept. of Neurology, Medical University of Vienna, Austria; [5]Dept. of Radiopharmaceuticals, Austrian Research Centers, Seibersdorf, Austria

Introduction: *R*-[[11]C]verapamil is a PET tracer for P-glycoprotein (P-gp) mediated transport at the blood-brain barrier. In humans, *R*-[[11]C]verapamil is metabolized via *N*-demethylation and *N*-dealkylation[1]. These metabolic pathways generate polar radiolabeled metabolites (e.g. [[11]C]formaldehyde) and via *N*-dealkylation, lipophilic [11]C-labeled metabolites, which are P-gp substrates.[2] A 1-tissue compartment model with the sum of *R*-[[11]C]verapamil and its *N*-dealkylation metabolites in arterial plasma as input function has been identified as the model of choice for kinetic analysis of *R*-[[11]C]verapamil.[2] The aim of this study was to assess peripheral *R*-[[11]C]verapamil metabolism in patients with temporal lobe epilepsy and compare these data with previously reported data from healthy volunteers.[1]

Experimental: 9 patients (43±9 years) underwent dynamic *R*-[[11]C]verapamil PET scans after i.v. administration of about 400 MBq of *R*-[[11]C]verapamil (specific activity: >20 GBq/μmol). Arterial blood samples were collected and select samples were analyzed for radiolabeled metabolites using an assay that measures polar metabolites by solid-phase extraction (SPE) and lipophilic *N*-dealkylation metabolites by HPLC.[3]

Results and Discussion: Peripheral metabolism of *R*-[[11]C]verapamil was considerably faster in patients as compared to healthy volunteers (see table). Faster metabolism appeared to be mainly due to increased *N*-demethylation as the polar metabolite fraction was about 2-fold greater in patients.

Table 1. *R*[[11]C]verapamil and its radiolabeled metabolites in arterial plasma (% of total radioactivity) of epilepsy patients (n = 9). Values in patentheses are previously reported healthy volunteer data [1]

Time (min)	*R*[[11]C]verapamil	HPCL-[[11]C]metabolites	[[11]C]Polar fraction
3.6±0.0*	97.4±2.0	–	2.6±2.0
5.1±0.1*	92.2±5.0	–	7.8±5.0
10.2±0.4	69.2±13.1 (85.0±6.9)	14.6±7.7 (7.8±2.8)	15.1±5.8 (7.7±4.4)
20.1±0.0	51.7±10.2 (70.2±9.9)	22.6±4.1 (17.6±4.9)	25.7±6.6 (12.8±4.7)
30.3±0.6	40.9±7.1 (62.7±10.3)	30.8±3.6 (21.5±6.2)	28.3±4.8 (15.5±5.8)
40.4±0.3	38.2±9.8 (56.9±9.7)	31.6±5.9 (25.5±8.6)	30.2±6.9 (17.3±4.4)
60.3±0.1	26.1±6.4 (49.0±13.4)	35.1±4.2 (30.1±7.8)	38.8±7.3 (22.3±5.5)

*For the first 2 time points no HPLC was performed and the *R*[[11]C]verapamil fraction therefore also includes lipophilic metabolites.

Conclusion: Faster peripheral metabolism of *R*-[[11]C]verapamil in epilepsy patients may be caused by cytochrome P450 enzyme induction by antiepileptic drugs. Based on these data caution is warranted when using an averaged arterial input function derived from healthy volunteers for the analysis of patient data. Moreover, our data illustrate how antiepileptic drugs may decrease serum levels of concomitant medication, which may eventually lead to a loss of therapeutic efficacy.

References: [1] Toornvliet R *et al* Clin Pharmacol Ther 79:540-8 (2006). [2] Lubberink M *et al* J Cereb Blood Flow Metab doi: 10.1038/sj.jcbfm.9600349 (2006). [3] Luurtsema G *et al* Nucl Med Biol 32:87-93 (2005).

Keywords: R-[[11]C]verapamil, PET, Metabolism, Antiepileptic Drugs

COMPARISON OF RADIOACTIVE METABOLITES OF ([18]F)FLUMAZENIL AND ([11]C)FLUMAZENIL IN HUMAN PLASMA

A.J. AIRAKSINEN [1], P. TRUONG [1], G. JOGOLEV [1], A. AMIR [1], R.N. KRASIKOVA [2] and C. HALLDIN [1]

[1]Department of Clinical Neuroscience, Karolinska Institutet, Stockholm, Sweden; [2]Institute of Human Brain, Russian Academy of Science, St. Petersburg, Russian Federation

Introduction: [^{11}C]Flumazenil is a widely used PET tracer for quantitative evaluation of central benzodiazepine receptors in human brain. [^{18}F]Flumazenil is a natural analogue of the native structure, and recently, its radiosynthesis via direct nucleophilic [^{18}F]fluorination of its nitro-precursor was reported, enabling production of [^{18}F]Flumazenil with high specific radioactivity (Ryzhikov NN et al. 2005; Windhorst AD et al. 2001).

The longer half life of ^{18}F may give more accurate analysis of its metabolites during a PET scan. The main metabolic pathway of flumazenil yields to its more hydrophilic acid metabolite Ro 15-3890, the main radioactive metabolite of both [^{18}F]Flumazenil and [^{11}C]Flumazenil (Debruyne D et al. 1991; Swahn C-G et al.1989; Halldin et al.1995).

Experimental: Radioactive metabolites of [^{18}F]Flumazenil and [^{11}C]Flumazenil were analyzed in healthy volunteers ([^{18}F]Flumazenil n = 10, [^{11}C]Flumazenil n = 5). Arterial blood samples were collected after i.v. injection of [^{18}F]Flumazenil at 4, 6, 8, 10, 20, 30, 40, 50, 60, 75, and 90 minutes and after i.v. injection of [^{11}C]Flumazenil at 4, 10, 20, 30, 40, 50 and 60 minutes. Blood was centrifuged, plasma proteins precipitated with acetonitrile and the supernatant was analyzed with gradient HPLC.

Results and Discussion: The metabolite analysis showed two more hydrophilic metabolites for the both tracers, the main metabolite [^{11}C/^{18}F]Ro 15-3890 and an unknown minor metabolite, which was not identified, but may correspond to the intermediate in the same metabolic pathway ([^{11}C/^{18}F]Ro 15-4965).

For [^{11}C]Flumazenil the amount of the parent compound gradually decreased until 20 min (30 ± 3%) after which the level of the intact parent compound remained stable. [^{18}F]Flumazenil showed slow decrease in [^{18}F]Flumazenil level during the whole observation time of 90 minutes (from 38 ± 1% at 20 min to 27 ± 3% at 90 min).

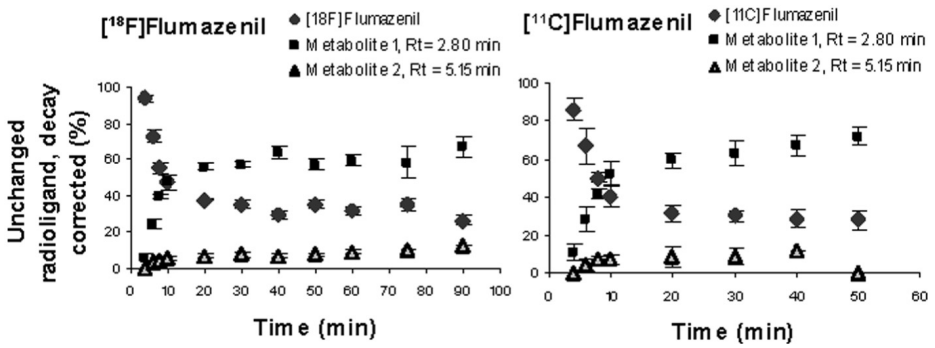

Conclusion: As conclusion, the metabolite pattern and rate of metabolism of [^{18}F]Flumazenil and [^{11}C]Flumazenil were similar. The longer half life of ^{18}F enables more accurate analysis of the amount of non metabolized parent compound.

Keywords: Benzodiazepine Receptors, Flumazenil, Human Plasma, Metabolites

PREPARATION, IN VITRO AND IN VITRO EVALUATION OF 8-(^{123}I)IODO-L-1,2,3,4-TETRAHYDRO-7-HYDROXYISOQUINOLINE-3-CARBOXYLIC ACID AS AN IMAGING AGENT FOR PROSTATE CANCER

C. FOZING [1], M. WAGNER [2], M.D. MENGER [3], C.M. KIRSCH [1] and S. SAMNICK [1]

[1]Nuclear Medicine, Saarland University Medical Center, Homburg, Saarland, Germany; [2]General Pathology, Saarland University Medical Center, Homburg, Saarland, Germany; [3]Clinical Experimental Surgery, Saarland University Medical Center, Homburg, Saarland, Germany

Introduction: Very few tracers are currently available for detection and staging of prostate cancer with PET and SPECT. This study evaluates the potential of 8-[^{123}I]iodo-1,2,3,4-tetrahydro-7-hydroxyisoquinoline-3-carboxylic acid [ITIC(OH)] as an imaging probe for detecting prostate cancer.

Experimental: No-carrier-added ITIC(OH) was synthesized by the IODO-GEN method with 82 ± 7% radiochemical yield and > 99% radiochemical purity after HPLC. Thereafter, tumor affinity and uptake characteristics of ITIC(OH) were assessed *in vitro* in human PC-3 and DU-145 prostate tumor cells. In addition, ITIC(OH) was examined in CD1 nu/nu mice engrafted with PC-3 and DU-145 prostate cancer in the flank or orthotopically in the prostate as experimental models of human prostate cancer. The bioevaluation included the examination of the *in vivo* stability and measurements of the uptake kinetic in tumors and organs of interest by dynamic imaging using a high resolution gamma-camera as well as biodistribution by gamma-counting after dissection.

Results and Discussion: The uptake of ITIC(OH) in primary human prostate tumor cells was rapid. More than 80% of the total radioactivity accumulation in cells occurred in the first 2-3 min. The uptake in 10^6 tumor cells after a 15 min-incubation time was 35–42% of the total loaded dosis. In vivo, ITIC(OH) accumulates rapidly and with high intensity in human prostate tumor xenografts after intravenous administration. At 60 and 240 min postinjection, the radioactivity binding in tumors amounted to 13.6 ± 2.1 and 16.2 ± 2.5% I.D./g in the heterotopic tumors compared with 14.8 ± 2.6 and 17.6 ± 3.4% I.D./g in the orthotopic tumor engrafts. (In contrast, radioactivity uptake in blood, spleen, liver and gastrointestinal tract was moderate and decreased with time, resulting to a marked tumor-to-background and an excellent visualization of the tumors). The resulting mean tumor-to-organ ratios at 60 and 240 min were 22.2 ± 4.7 and 48.4 ± 6.6 (tumor/blood), 21.7 ± 4.4 and 26.5 ± 6.6 (tumor/muscle), 13.4 ± 3.1 and 27.6 ± 7.5 (tumor/spleen), 2.3 ± 0.7 and 3.9 ± 1.6 (tumor/kidney), 5.2 ± 1.1 and 6.9 ± 2.3 (tumor/intestine), as well as 4.2 ± 1.3 and 13.2 ± 3.5 (tumor/liver).

Conclusion: These results suggest that ITIC(OH) is a promising candidate as radiotracer for detecting prostate cancer and warrant further studies in patients to ascertain its potential as an imaging agent for clinical use.

Keywords: Prostate Cancer, Experimental Tumor Models, Unnatural Amino Acids, Pharmacokinetics, Preclinical Study

COMPARATIVE *IN VIVO* EVALUATION OF EGFR-TARGETING AFFIBOY MOLECULES

A. ORLOVA [1,2], M. FRIEDMAN [3], M. SANDSTRÖM [4], T.L. ERIKSSON [1], S. STÅHL [3], F.Y. NILSSON [1,2] and V. TOLMACHEV [1,2,5]

[1]Affibody AB, Bromma, Sweden; [2]Unit of Biomedical Radiation Sciences, Uppsala University, Uppsala, Sweden; [3]School of Biotechnology, Royal Institute of Technology, Stockholm, Sweden; [4]Section of Hospital Physics, Uppsala University Hospital, Uppsala, Sweden; [5]Department of Medical Sciences, Nuclear Medicine, Uppsala University, Uppsala, Sweden

Introduction: The epidermal growth factor receptor (EGFR) is a target for a number of novel anticancer therapies. Selection of patients who will benefit from these therapeutics may be done by imaging of a EGFR-expression. Affibody molecules are small (7 kDa) proteins which can be selected for high affinity binding to protein targets. The goal of this study was to evaluate the use of the anti-EGFR Affibody molecule Z_{1907} for imaging of EGFR expression in a murine xenograft model.

Experimental: The anti-EGFR Affibody molecule Z_{1907} posess an affinity to EGFR of 5.3 nM. Both the monomeric form Z_{1907} and the dimeric form $(Z_{1907})_2$ were produced in *E. coli*. Proteins were labelled with ^{111}In using isothiocyanate-benzyl-DTPA (^{111}In-Bz-DTPA) and with ^{125}I using succinimidyl -*para*-iodo-benzoate (^{125}I –PIB). A comparative biodistribution study in nude mice bearing A431 xenografts was performed 4 and 24 h pi. Specificity of a tumour uptake was confirmed using size-matched non-cancer specific Affibody molecules, which were labelled using the same techniques.

Results and Discussion: Labelling yields were of about 90% for ^{111}In, and about 40% for ^{125}I. In vitro cell binding tests showed that all conjugates, ^{111}In-Bz-DTPA-Z_{1907}, ^{111}In-Bz-DTPA-$(Z_{1907})_2$, ^{125}I-PIB-Z_{1907} and ^{125}I-PIB-$(Z_{1907})_2$, retained capacity to bind specifically to EGFR-expressing A431 cervical carcinoma cells. The use of ^{111}In-labelled Affibody molecules resulted in better tumour accumulation in vivo compared with the radioiodinated ones. Despite lower affinity, the tumour uptake of the monomeric forms was higher, presumably due to better extravasation and tumour penetration. The dimeric forms resulted in higher accumulation and retention of radioactivity in liver. At later time points, washout of the radioactivity from both tumours and normal tissues was observed for both di-and monomeric forms. However, the washout was more rapid from normal tissues, which increased tumour-to-non tumour ratios. The best tumour-targeting results were obtained using ^{111}In-Bz DTPA-Z_{1907}, which provided a tumour uptake of 2.02±0.32%IA/g, tumour-to-blood ratio of 31±9 and tumour-to-iver ratio of 1.8±0.4 at 24 h pi. Gamma-camera imaging (24h pi) showed a clear visualisation of xenografts using ^{111}In-Bz-DTPA-Z_{1907}.

Conclusion: In conclusion, the^{111}In-Bz-DTPA-Z_{1907} is a promising Affibody tracer for visualisation of EGFR expression in tumours.

Acknowledgement: This work was supported by grants from Swedish Cancer Society and VINNOVA.

Keywords: EGFR, Affibody Molecule, In-111, I-125, Molecular Imaging